Periodic solutions and chaotic attractors of a modified epidemiological SCIS model

Michael Bestehorn, Thomas M. Michelitsch

Periodic solutions and chaotic attractors of a modified epidemiological SCIS model

Michael Bestehorn

Brandenburgische Technische Universität Cottbus-Senftenberg,

Institut für Physik,

Erich-Weinert-Str. 1,

03046 Cottbus, Germany,

orcid: 0000-0002-3152-8356

bestehorn@b-tu.de

Thomas M. Michelitsch

Sorbonne Université, Institut Jean le Rond d'Alembert,

CNRS UMR 7190, 4 place Jussieu,

75252 Paris cedex 05, France, orcid: 0000-0001-7955-6666

thomas.michelitsch@sorbonne-universite.fr

Abstract

We consider a generalized SCIS model where individuals are divided into the three compartments **S** (healthy and susceptible), **C** (infected but not just infectious) and **I** (infectious). Finite waiting times in the compartments yield a system of delay-differential or memory equations and may exhibit oscillatory (Hopf) instabilities of the otherwise stationary endemic state, leading normally to regular oscillations in the form of an attractive limit cycle in the phase space spanned by the compartment rates.

In the present paper our aim is to demonstrate that in the dynamics of delayed SCIS models persistent chaotic attractors can bifurcate from these limit cycles and become accessible if the nonlinear interaction terms fulfill certain basic requirements. Computing the largest Lyapunov exponent we show that chaotic behavior exists in a wide parameter range.

Finally, we discuss a more general system and show that a sudden falloff of the infection rate with respect to increasing infection number may be responsible for the emergence of chaotic time evolution. Such a falloff can describe mitigation measures like wearing masques, individual isolation or vaccination. The model may have a wide range of interdisciplinary applications beyond epidemic spreading for instance in the kinetics of certain chemical reactions.

Keywords: Epidemic spreading, memory effects, generalized SIR models, chaotic attractors

I. INTRODUCTION

Beginning with the book of Thomas Robert Malthus in 1798 [1], the modeling of population dynamics has a long tradition. The nowadays called 'Malthusian growth model' was later generalized by F. J. Richards [2] and others. Predator-Prey systems where studied from 1925 by Lotka and Volterra [3, 4]. The seminal work of Kermack and McKendrick [5] in 1927 where the nowadays called 'SIR model' was introduced can be seen as the initiation of epidemic models. Being a specialization of a predator-prey system, the original SIR equations have obtained many extensions and modifications. A huge number of publications exists based on this model which is built on a low-dimensional system of ordinary differential equations, for a review see [6].

SIR models refer to the class of compartmental models'' since they divide the individuals into several compartments depending on their state of health. In this way, SIR stands for an acronym from ($\mathbf{S}$ = susceptible, $\mathbf{I}$ = infected, $\mathbf{R}$ = recovered). It turned out that the features of infectious diseases such as measles, mumps, and rubella could to a certain extent be captured by such simple models.

On the other hand, all these diseases come in waves with a more or less regular periodicity. The waves can be triggered by external reasons like seasons, but also by some internal mechanisms. Such an intrinsic behavior was already speculated in 1929 by Soper in a model for the time evolution of measles cases [7].

In the standard SIR models, the interplay between infected and susceptible individuals is inspired by an interaction of the predator-prey kind where the infection rate is expressed in the form of a simple bilinear term $\beta_0\, j(t)\, s(t)$. Here, $j(t)$ and $s(t)$ are the relative number of infected ($\mathbf{I}$) and susceptible ($\mathbf{S}$) individuals and β_0 is related to the constant probability of infection at each contact (infection rate). The predator (infected) 'catches' the prey (susceptible) by infection. Predator-prey models of the classical SIR type are not able to describe sustained oscillations that originate from the instability of a fixed point, here the endemic equilibrium, but rather account for single outbreaks if the healthy state becomes unstable. In the long time limit, herd immunity and the endemic equilibrium as a stable fixed point is reached where the fractions of the population in the different compartments attain constant values. However, it turns out that there is a further class of predator-prey models with modified infection rates $A(s(t), j(t))$ and delayed transitions exhibiting

oscillatory instabilities and routes to chaos.

Other work [8] considered a nonlinear infection rate according to

$$A(s,j) = \beta(j)\, j(t)\, s(t) = \frac{\beta_0\, j^m(t)\, s(t)}{1+\alpha j^n(t)} \ , \tag{1}$$

and obtain limit cycle solutions for certain parameters $m = n \geq 2,\ \alpha > 0$. Tang et al. [9] studied the case $m = n = 2$ and found a weak focus and the existence of two limit cycles. For $m = n = 1$ the dynamics is qualitatively the same than for the standard SIR model and sustained oscillations cannot be observed. The denominator $1+\alpha j^n$ accounts for mitigation measures against the epidemics that naturally increase with increasing j. Note that for the case $n > m$ the interaction A has a maximum at a certain infection number. For such non-monotonic behavior it was shown in [10] that the dynamics in the long time limit approaches a stable fixed point as for the original SIR models.

In earlier work we showed that a finite (long) immunity life-time [11] as well as delayed mitigation measures [12] lead to a system of delay-differential or memory equations and may show oscillatory instabilities of the otherwise endemic state, leading to normally regular oscillations of the compartment rates. Memory terms were introduced in epidemiological models by many other researchers, for an overview see [13]. From the mathematical point of view, the presence of a delay term in an ordinary differential equation makes a low-dimensional system infinitely dimensional and may allow for the occurrence of periodic, quasi-periodic or even chaotic behavior, rendering the dynamics much more complex [14–16].

A crucial element of our extended model studied in the present paper is the introduction of a class of infection rate functions exhibiting a sudden falloff with respect to the infection numbers, according to (1) for large enough n. We demonstrate that the complex interplay of these kinds of infection rates and delayed transitions between the compartments is the actual source of the chaotic dynamics. The well known Mackey-Glass equations [17] refers to our model class and we show in section IV that the Mackey-Glass eqs. can be derived systematically from our model for the approximation of a constant susceptibility rate. However, our model generalizes the Mackey-Glass system in two respects. Firstly it highlights the interpretation as a compartmental model and considers continuously distributed compartmental waiting time distributions for the delayed transitions, and secondly it admits a wide range of infection rate functions (beyond the one used in the Mackey-Glass model)

with the above mentioned falloff feature. To the best of our knowledge there is so far no such approach in epidemic modeling.

Our aim is to develop a model as close as possible to the non-delayed standard models. For further sake of simplicity, we consider first only two compartments, namely **S** and **I**, and assume that recovered individuals transfer directly back to the **S** compartment, leading to an SIS model. The crucial point is that the infection **S** to **I** is assumed to take a certain finite time. This can be modeled by introducing a new compartment **C** where the individuals are already infected but not yet infectious (incubation phase). Thus we shall consider here a SCIS model with finite delay times for the transitions C $\rightarrow$ I and I $\rightarrow$ S, respectively.

The paper is organized as follows: In sect. 2 we introduce the SCIS model for general distributions of the waiting times in the different compartments. Equilibrium points and their stability are given and examined in more detail for δ-shaped kernel functions, leading to a set of two coupled delay differential equations for the fractions of **S** and **I**. The critical conditions for a Hopf bifurcation are determined analytically. In sect. 3, numerical solutions of delay system are computed and the emergence of a chaotic attractor is demonstrated, its largest Lyapunov exponent is found to be positive for large regions of the basic reproduction number. In sect. 4 the analogy to the Mackey-Glass system is shown for the approximation of a constant susceptible population. A mechanism for the occurrence of chaotic attractors is proposed.

II. THE MODEL

A. Generalized SIRS model with memory

In the present paper we shall consider a generalized SCIS model without birth or death processes, leading to a constant total population of N individuals. According to their state of health, the individuals are divided into the three compartments **S** (healthy and susceptible), **C** (infected but not just infectious) and **I** (infectious), see Fig. 1, with the total population number $N = S + C + I$.

We define the fractions

$$s(t) = S(t)/N, \quad c(t) = C(t)/N, \quad j(t) = I(t)/N$$

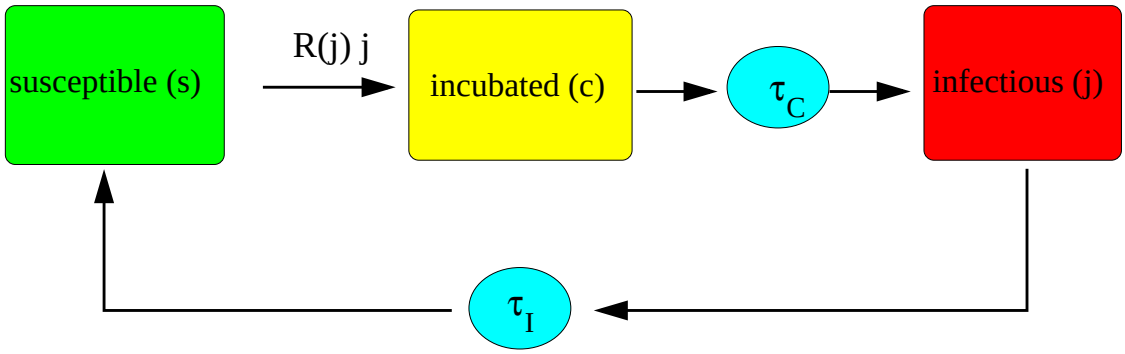

FIG. 1: The SCIS model with a j-dependent basic reproduction number $R(j)$ and finite (random) delay times τ_C, τ_I between compartments **C**, **I** and **I**, **S**, respectively.

with $s + c + j = 1$. The model reads

$$\frac{ds}{dt} = -A(t) + \langle A(t - \tau_C - \tau_I)\rangle \tag{2a}$$

$$\frac{dc}{dt} = A(t) - \langle A(t - \tau_C)\rangle \tag{2b}$$

$$\frac{dj}{dt} = \langle A(t - \tau_C)\rangle - \langle A(t - \tau_C - \tau_I)\rangle \tag{2c}$$

where $A(t)$ indicates the infection rate which describes the nonlinear interaction at time t. The delay time τ_C between the instant of infection (transition S $\to$ C) and transition C $\to$ I has the interpretation of an incubation time. The incubation time is followed by the sojourn time τ_I in compartment I where the individual is infected and infectious (ill). After spending the time τ_I in compartment I, the individual recovers, undergoing a transition I $\to$ S.

Considering the transitions occurring at time instant t gives an evocative interpretation of eqs. (2): $A(t)$ indicates the infections (transitions S $\to$ C) at instant t. The term $A(t - \tau_C)$ accounts for the past infections at $t - \tau_C$ for which at instant t the incubation time has elapsed and which undergo a transition C $\to$ I at instant t, see (2b,2c). Further, the term $A(t - \tau_C - \tau_I)$ comes from the infections that happened in the past at instant $t - \tau_C - \tau_I$ for which at time t both, the incubation time τ_C and the illness time τ_I have elapsed and hence are recovering at instant t with transition I $\to$ S, see (2c,2a). In eqs. (2), $\langle \ldots \rangle$ stands for the means with respect to the independent random times τ_C and τ_I drawn from the normalized

PDFs (memory functions) $K_C,\ K_I$ and are computed from

$$\begin{aligned}\langle A(t-\tau_C)\rangle &= \int_0^t K_C(t-\tau)A(\tau)\mathrm{d}\tau \\ \langle A(t-\tau_C-\tau_I)\rangle &= \int_0^t\int_0^\tau K_I(t-\tau)K_C(\tau-\tau')A(\tau')d\tau' d\tau\end{aligned}$$

We note that the system (2) is included in the more general case of a SCIRS cycle, examined in detail in a recent paper [16].

For the interaction A that models the infection rate we consider the class

$$A(t) = A(s(t), j(t)) = R_0\, s(t)\, j(t)\, f(j(t)) \tag{3}$$

with a monotonically decreasing function

$$f(j) = \frac{1}{1+\alpha^n j^n}$$

with some positive α and integer $n > 1$, according to (1). This leads to a decrease of the effective basic reproduction number if j is increasing and vice versa, modeling mitigation measures like containment, masques, etc. Note that A has a maximum at

$$j_m = \frac{(n-1)^{1/n}}{\alpha} \approx \frac{1}{\alpha} \quad \text{for } n \gg 1\ .$$

Instead of studying the full system (2) we assume an exponential distribution for K_I according to

$$K_I(\tau) = \gamma \exp(-\gamma\tau) \tag{4}$$

that has the mean value $\langle\tau_I\rangle = 1/\gamma$. It can be easily seen by differentiation that for such a PDF the relation

$$\langle A(t-\tau_C-\tau_I)\rangle = \gamma\,(j(t)-j(0))$$

holds. Since c is not occurring explicitly, it is sufficient to consider eqs. (2a,2c). Scaling time with $t = t'/\gamma$ and substituting (4) with $j(0) = 0$ yields the two coupled memory equations

$$\frac{ds}{dt'} = -R_0' \frac{sj}{1+\alpha^n j^n} + j \tag{5a}$$

$$\frac{dj}{dt'} = R_0' \int_0^t d\tau'\, K_C(t-\tau')\frac{s(\tau')j(\tau')}{1+\alpha^n j^n(\tau')} - j \tag{5b}$$

with $R_0' = R_0/\gamma,\ \tau' = \tau\gamma$. In the following, we shall leave all primes and time is measured in units of the time of recovery. The standard SIS model is recovered for $\alpha = 0$ and $K_C(\tau) = \delta(\tau)$. For $K_C(\tau) = \delta(\tau-\tau_C)$ one has a sharp delay time τ_C for the incubation period. This is a special case that will be treated in sect. II C in more detail.

B. Equilibrium points and their stability

There are two equilibrium solutions or fixed points of (5). The first one is the state before the epidemic breaks out (healthy state) and reads

$$s_h = 1,\ j_h = 0\ . \tag{6}$$

The other one is the endemic equilibrium found from

$$A = j_e, \qquad s_e = 1 - j_e\,(1 + \langle\tau_C\rangle) \tag{7}$$

or

$$\alpha^n j_e^n + j_e R_0\,(1 + \langle\tau_C\rangle) + 1 - R_0 = 0\ , \tag{8}$$

where we used $j_e + s_e + c_e = 1$ and $c_e = A\,\langle\tau_C\rangle$.

We compute the stability of both equilibrium points applying linear stability analysis. Inserting

$$s(t) = s_0 + u\,\mathrm{e}^{\lambda t}, \quad j(t) = j_0 + v\,\mathrm{e}^{\lambda t}$$

where $s_0,\ j_0$ stands for the equilibrium point in (5) yields a linear system that has the transcendental equation

$$\lambda^2 + \lambda\left(a - b\,\hat{K}_C(\lambda) + 1\right) + a\left(1 - \hat{K}_C(\lambda)\right) = 0 \tag{9}$$

as solvability condition. Here,

$$a = \left.\frac{\partial A}{\partial s}\right|_{s_0,j_0} = \frac{R_0 j_0}{1 + \alpha^n j_0^n} \tag{10a}$$

$$b = \left.\frac{\partial A}{\partial j}\right|_{s_0,j_0} = \frac{R_0 s_0}{1 + \alpha^n j_0^n} - \frac{R_0 n s_0 \alpha^n j_0^n}{(1 + \alpha^n j_0^n)^2} \tag{10b}$$

and $\hat{K}_C$ as Laplace transform of K_C:

$$\hat{K}_C(\lambda) = \int_0^\infty dt\, K_C(t)\,\mathrm{e}^{-\lambda t}\ . \tag{11}$$

Note that R_0 is retrieved from $R_0 = \left.\dfrac{\partial A}{\partial j}\right|_{s=1,j=0}$. The state (6) yields $a = 0,\ b = R_0$ and from (9)

$$\lambda = R_0\,\hat{K}_C(\lambda) - 1\ .$$

The critical point is $\lambda = 0$. Expanding (11) yields

$$\hat{K}_C = \int_0^\infty dt\, K_C(t)\,(1-\lambda t) + O(\lambda^2) = 1 - \lambda\langle\tau_C\rangle + O(\lambda^2)$$

and in linear order

$$\lambda = \frac{R_0 - 1}{1 + R_0\langle\tau_C\rangle}\ .$$

Thus, the healthy state is is stable for $R_0 < 1$ and becomes an unstable saddle node for $R_0 > 1$.

C. Delay equations

For the special case of a δ-shaped kernel, one has

$$\hat{K}_C(\lambda) = \mathrm{e}^{-\lambda\tau_C}$$

and (5) turns into a system of delay differential equations:

$$\frac{ds}{dt} = -R_0\,\frac{sj}{1+\alpha^n j^n} + j \tag{12a}$$

$$\frac{dj}{dt} = R_0\,\frac{s(t-\tau_C)j(t-\tau_C)}{1+\alpha^n j^n(t-\tau_C)} - j\ . \tag{12b}$$

For $\tau_C = 0$, $\hat{K}_C = 1$ and the endemic equilibrium has the two eigenvalues

$$\lambda = 0, \qquad \lambda = b - a - 1\ .$$

The first one belongs to a marginal (Goldstone) mode that describes a shift between j_e and s_e, since for $\tau_C = 0$ the sum of the two equations (12) yields $d_t(s+j) = 0$. The second eigenvalue is always negative and the stability of the endemic state is proven without restrictions.

If $\tau_C > 0$, a Hopf instability becomes possible and (9) can be solved with $\lambda = i\omega$, leading to

$$\omega^2 = b^2 - a^2 - 1 \tag{13}$$

and

$$\tau_H = \frac{1}{\omega}\,\arccos\left[\frac{\omega^2(b-a+ba)+a^2}{a^2+b^2\omega^2}\right]\ . \tag{14}$$

Thus, the endemic equilibrium becomes unstable if τ_C exceeds τ_H with the critical frequency (13). Eq. (14) has to be solved iteratively because a, b depend on τ. Fig. 2 shows τ_H and the period $T = 2\pi/\omega$ over R_0.

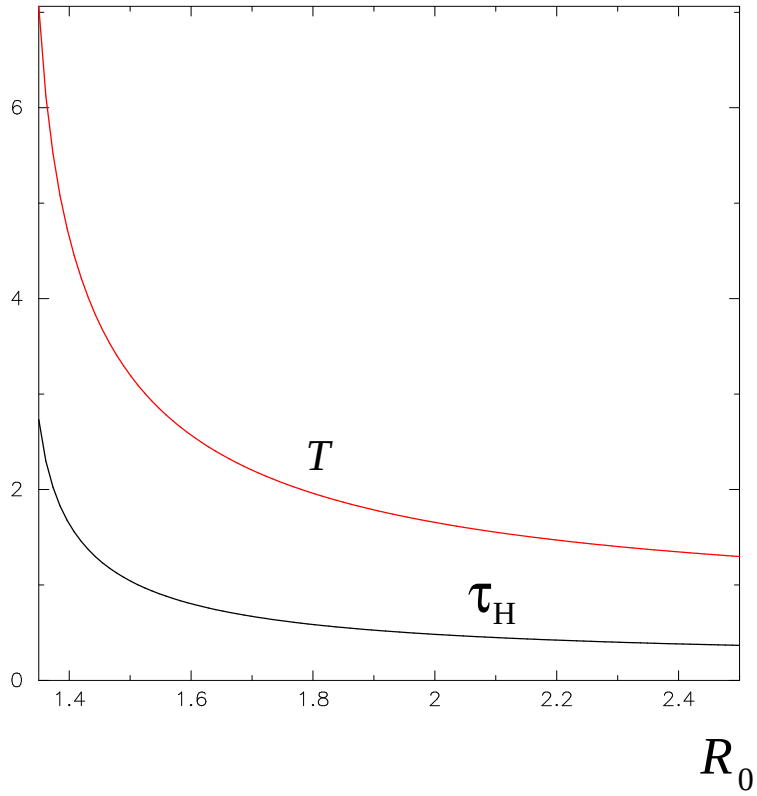

FIG. 2: Critical delay time necessary for an oscillatory instability of the endemic equilibrium and period of Hopf frequency (red).

III. RESULTS

A. Numerical solutions of the delay-differential system

We solved the nonlinear delay system by a standard 4th order Runge-Kutta method with fixed time step $\delta t = 10^{-4}$, for details see [18].

For large values of n, j_e becomes an unstable focus if τ_C exceeds a critical value. For even larger delay times, a chaotic attractor emerges. Fig. 3 shows a time series for the periodic case with

$$R_0 = 2.5, \quad \alpha = 100, \quad \tau_C = 1, \quad n = 10$$

and for the chaotic case with $\tau_C = 2$.

Fig. 4, left frame, shows the chaotic attractor at $\tau_C = 2$ where $j(t)$ is plotted versus $j(t - \tau_C)$. In Fig. 4, right frame, the same attractor is plotted in the s-j phase plane.

Contrary to the standard SCIS model it is remarkable that the variation of s is very

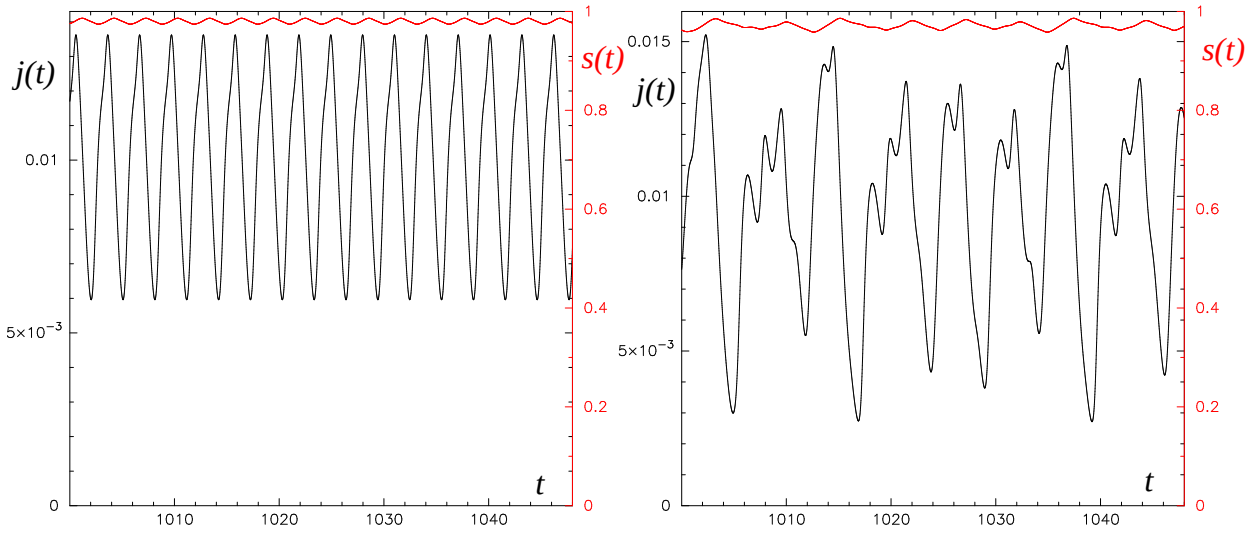

FIG. 3: $j(t)$ (black) and $s(t)$ (red) in the periodic (left frame) and in the chaotic (right frame) regime.

small. This agrees well with real world data for instance for COVID, where herd immunity was always far from being reached during or between the wave outbursts, see also [19].

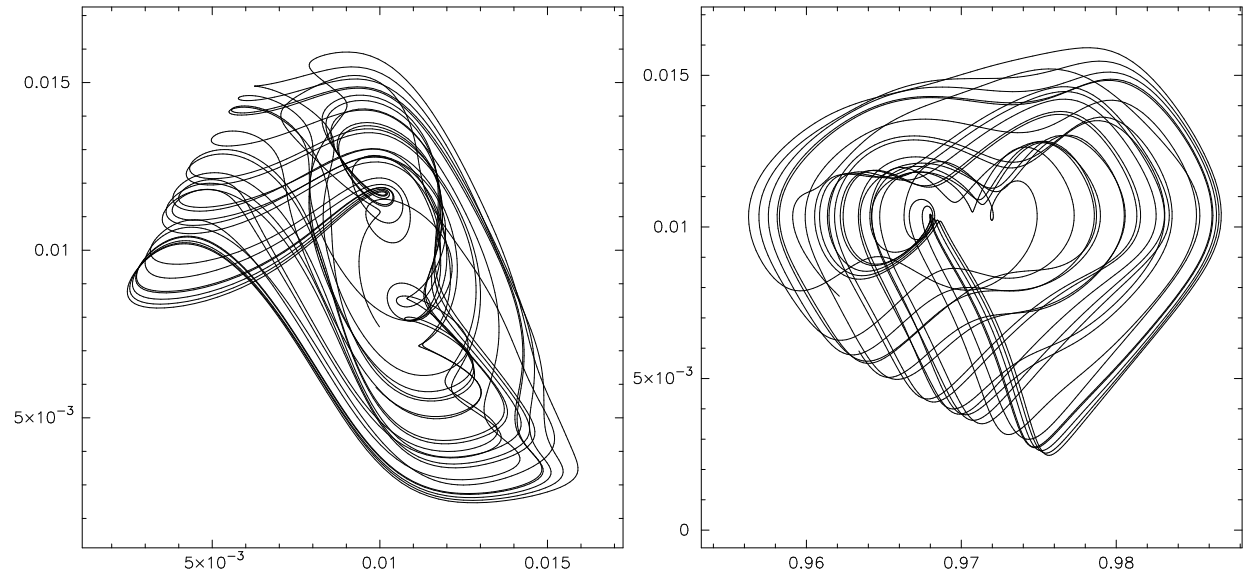

FIG. 4: Chaotic attractor for $\tau_C = 2$, left: $j(t)$ over $j(t - \tau_C)$, right: $j(t)$ over $s(t)$.

B. Lyapunov exponent

To demonstrate that the attractors found are really chaotic, we compute the largest Lyapunov exponent for two different values of τ_C. First, a main trajectory $s_0(t)$, $j_0(t)$ is

computed iterating (5) by a Runge-Kutta method, then the system is linearized with respect to the main trajectory

$$s(t) = s_0(t) + u(t), \qquad j(t) = j_0(t) + v(t)$$

From $t_0 = 4000$, the linear delay system

$$\frac{du}{dt} = -a(t)\, u(t) + (1 - b(t))\, v(t) \tag{15a}$$

$$\frac{dv}{dt} = a(t - \tau_C)\, u(t - \tau_C) + b(t - \tau_C)\, v(t - \tau_C) - v(t) \tag{15b}$$

is solved numerically by the same Runge-Kutta scheme. The chaotic time dependent functions a, b are obtained from (10) by replacing $j_0,\ s_0$ by $s_0(t),\ j_0(t)$. Starting with a normalized random initial condition

$$u(t) = \xi_t, \quad v(t) = \eta_t, \quad \int_{-\tau_C}^{0} dt\, (u^2 + v^2) = 1, \qquad t = [-\tau_C, 0]$$

where $\xi_t\ \eta_t$ are independent equally distributed random variables in [-0.5,0.5], the L^2 norm

$$R_k = \left[\int_{(k-1)\tau_C}^{k\tau_C} dt\, (u^2 + v^2) \right]^{1/2}, \qquad k = 1, 2, ...$$

is computed each time after t reaches $k\tau_C$ and (u, v) is normalized again, see e.g. [18]. This process is repeated until $t_e = 8000$ and the largest Lyapunov exponent is found according to

$$\Lambda = \frac{1}{t_e - t_0} \sum_k \ln(R_k)\ .$$

The result is shown in Fig. 5.

C. Memory equations

Next we study the system (5) with a kernel function of certain finite width. To this end we take the Erlang function defined as

$$K_C(\tau) = \frac{\xi^\beta}{\Gamma(\beta)}\, \tau^{\beta-1} \mathrm{e}^{-\xi\tau}, \qquad \beta = \xi\, \langle\tau\rangle = \xi\, \tau_0 \tag{16}$$

having a width $\sim 1/\xi$ and which approaches the δ-function $\delta(\tau - \tau_0)$ for $\xi \to \infty$, see Fig. 6. Fig. 7 shows some numerical solutions for different ξ. Chaotic attractors are only obtained if ξ exceeds a certain value that depends also on τ and R_0.

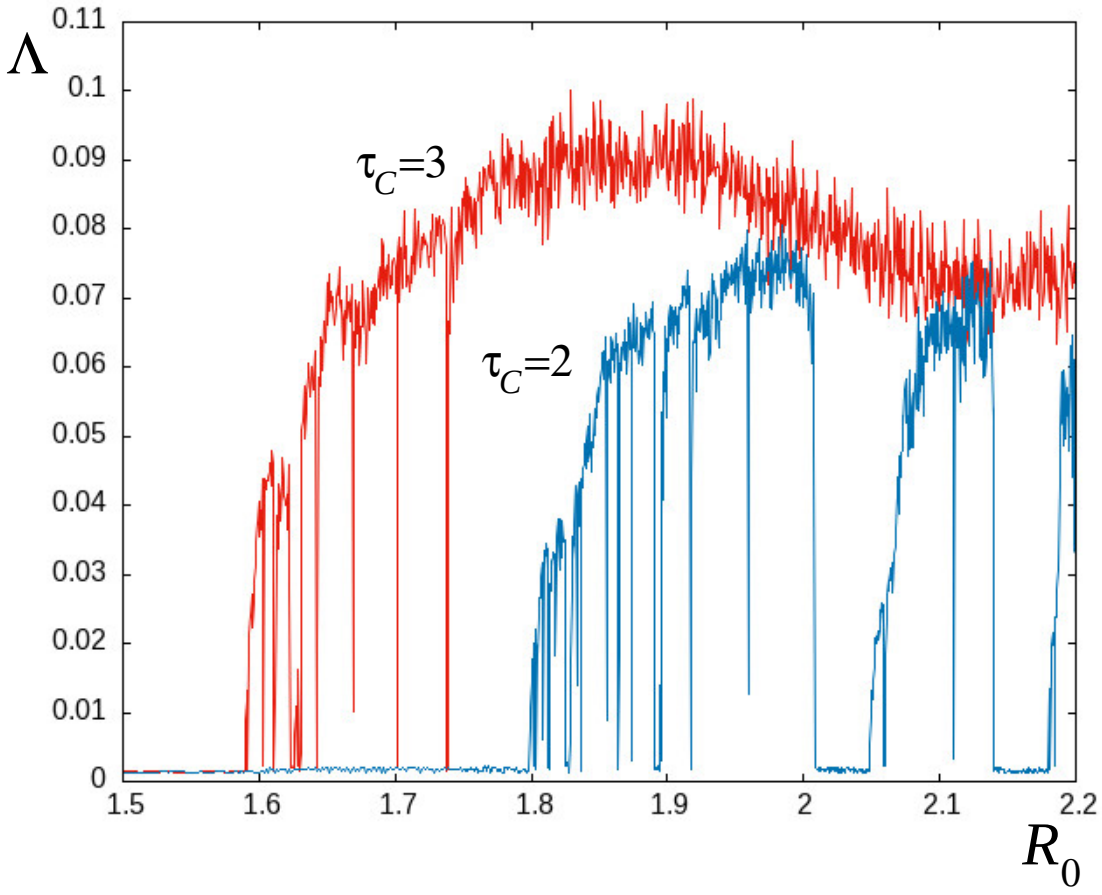

FIG. 5: Largest Lyapunov exponents for $\tau_C = 2$ (blue) and $\tau_C = 3$ (red), over R_0. Periodic windows can be clearly seen.

To demonstrate this more clearly we computed the largest Lyapunov exponent also for this case. Now, Eqs. (15) turn into the linear memory system

$$\frac{du}{dt} = -a(t)\,u(t) + (1 - b(t))\,v(t) \tag{17a}$$

$$\frac{dv}{dt} = \int_0^t d\tau\, K_C(t-\tau)\left[a(\tau)\,u(\tau) + b(\tau)\,v(\tau)\right] - v(t)\ . \tag{17b}$$

The rest of the procedure remains the same as described in sect. III B. The result for different ξ is shown in Fig. 8.

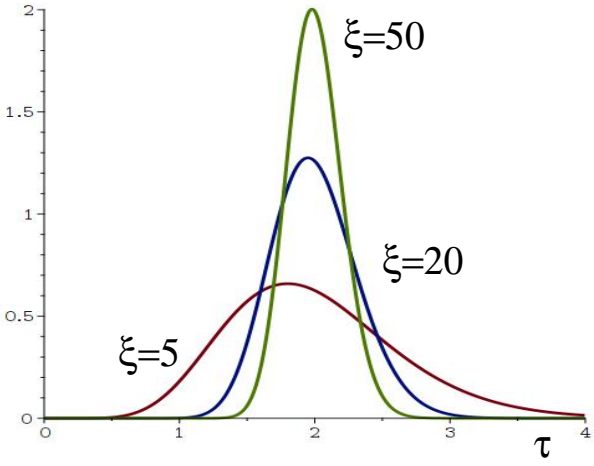

FIG. 6: Erlang functions (16) for $\tau_0 = 2$ and different ξ.

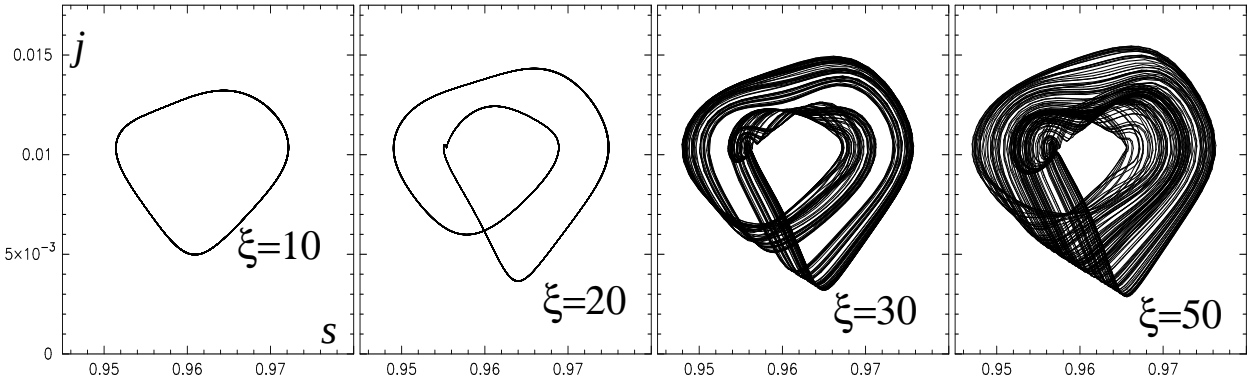

FIG. 7: Phase plots in the sj-plane for different ξ and $\tau_0 = 2,\ R_0 = 2.5$.

IV. MACKEY-GLASS EQUATION

Introducing the new variable $x(t) = \alpha j(t)$, eq. (5a) turns into

$$\frac{ds}{dt} = \frac{1}{\alpha}\left[-R_0\,\frac{sx}{1+x^n} + x\right] \ .$$

To have an effective feedback, αj should be of order one and since j is rather small, $\alpha \gg 1$. As a first approximation we may then put

$$\frac{ds}{dt} \approx 0, \qquad s = s_0 = \text{const.}$$

where s_0 is the initial value and therefore close to one. Then from (5b) we find immediately

$$\frac{dx}{d\tilde{t}} = \int_0^{\tilde{t}} d\tau\, K_C(\tilde{t}-\tau)\frac{x(\tau)}{1+x^n(\tau)} - \mu\, x \tag{18}$$

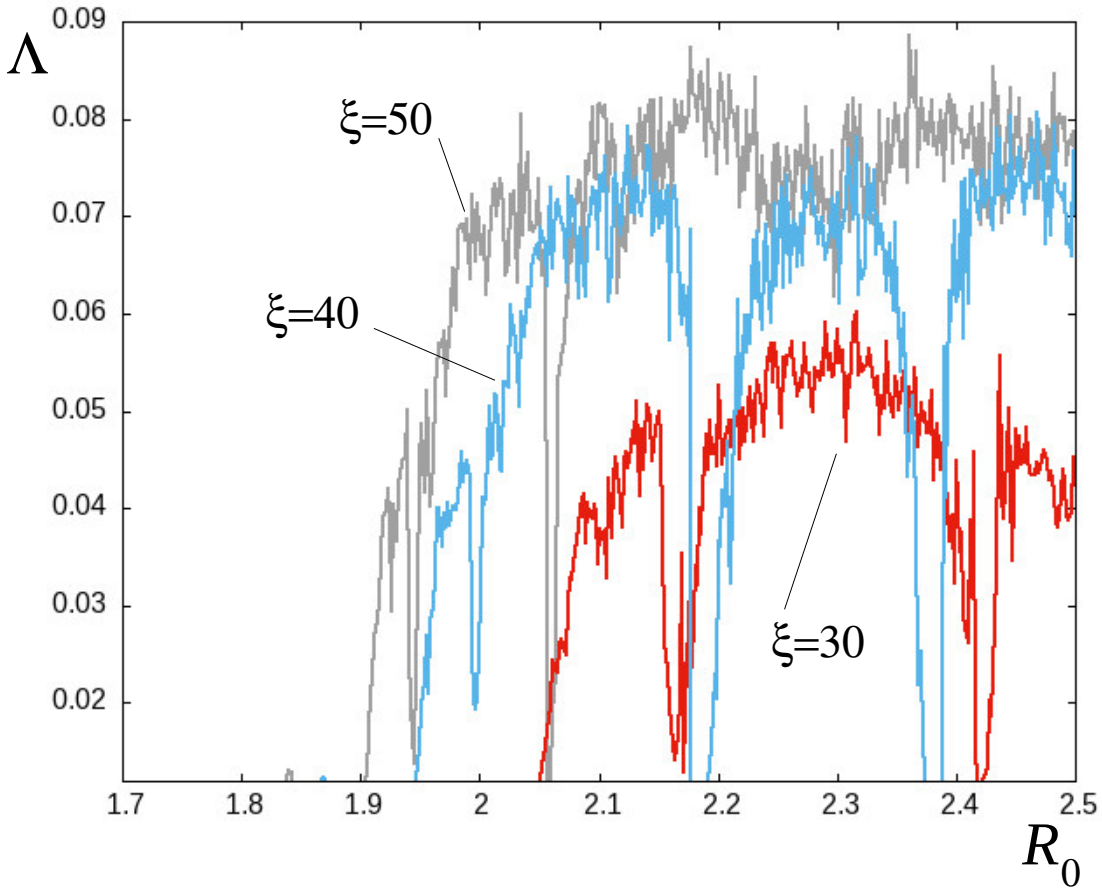

FIG. 8: Largest Lyapunov exponents for $\tau_0 = 2$ and the Erlang kernel (16) with $\xi = 50$ (gray), $\xi = 40$ (blue), $\xi = 30$ (red).

where time is scaled again with $t = \tilde{t}/R_0 s_0$ and $\mu = 1/R_0 s_0 < 1$.

Eq. (18) can be considered as a Mackey-Glass equation with memory. It turns into the original Mackey-Glass equation for a δ-kernel $K_C = \delta(\tau - \tau_0)$ and has the form (tildes removed)

$$\frac{dx}{dt} = \frac{x(t-\tau_0)}{1 + x^n(t-\tau_0)} - \mu\, x \ . \tag{19}$$

It is well-known since the remarkable paper of Mackey and Glass [17] who derived it as a model for the control of blood cell concentration that this equation has a chaotic attractor for rather large n and if τ_0 exceeds a certain critical value. The attractor is born after an oscillatory instability of the non-trivial fixed point followed by period doubling. The bifurcation scenario and the resulting trajectories have much in common with our solutions shown in Fig. 4, left frame.

Instead of (19) let us examine the more general delay equation

$$\frac{dx}{dt} = x(t-\tau)\, f(x(t-\tau)) - \frac{x}{2} \tag{20}$$

where f is a monotonically decreasing function with

$$f(0) = 1, \quad f(x \to \infty) = 0$$

and a certain more or less steep decrease close to $x = 1$. As a test function fulfilling all requirements we may choose

$$f(x) = \frac{1}{2}\left(1 + \tanh \beta(1-x)\right) \tag{21}$$

where $1/\beta$ denotes the width of the step. Then, (20) has an unconditionally unstable fixed point at $x = 0$ and a second one at $x = 1$ that is stable for $\tau < \tau_c$ and becomes an unstable focus at $\tau = \tau_c$. A linear analysis yields

$$\tau_c = \frac{1}{\omega_c} \arccos\left(\frac{1}{1-\beta}\right), \qquad \omega_c = \frac{1}{2}\sqrt{(1-\beta)^2 - 1} \tag{22}$$

with the Hopf frequency ω_c, fig. 9. A limit cycle occurs if τ exceeds τ_c, followed by several period doublings until eventually a chaotic attractor may emerge, see fig. 10. Thereby, the steepness β of (21) plays a crucial role. The threshold (22) only exists if $\beta > 2$. Moreover, if $f(x)$ is too flat, chaos never occurs or only for large delay times τ. The value $x = 1$ could be interpreted as a kind of separatrix. For $x > 1$ the delay term in (20) has no or only little effect and x decreases exponentially until the trajectory is back in the 'delay region' $x < 1$. Then the delay term determines again the dynamics and may throw x across the separatrix. This back and forth motion is sensible with respect to small perturbations and may be finally responsible for the chaotic nature of the trajectory.

V. CONCLUSIONS

Contrary to the standard SIR model and its various extensions, time-periodic trajectories occur in a natural way if the ordinary differential equations are not local in time but contain memory terms where the history of the evolution is included. We have shown that if these terms have a special form, chaotic solutions may exist that are not caused by fluctuations and thereby still deterministic. Starting from the most simple epidemic system containing

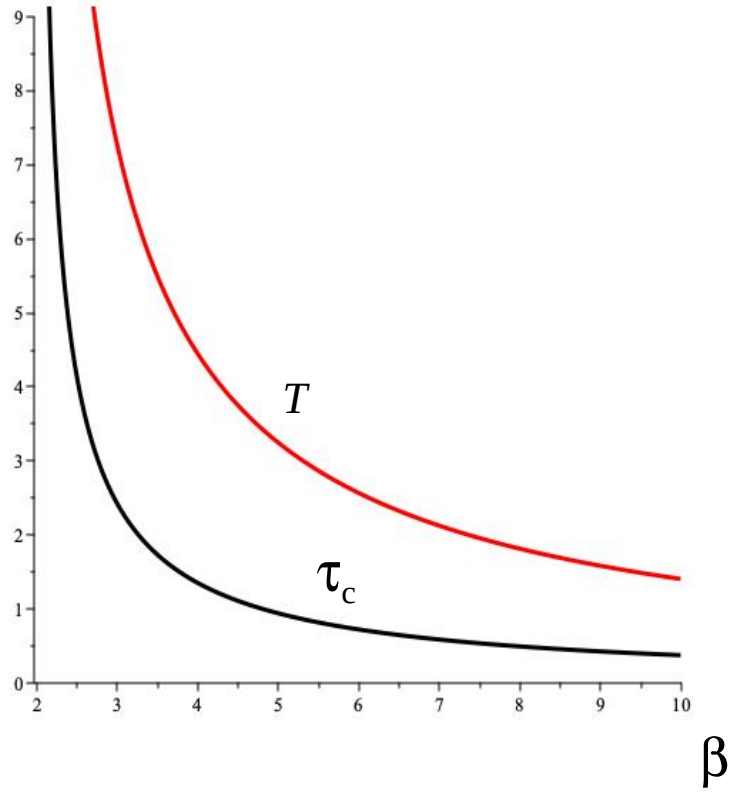

FIG. 9: Critical delay time necessary for an oscillatory instability according to (22) and period of Hopf frequency (red). Note the similarity to fig. 2.

only the two compartments for susceptible and infected individuals, we derived a minimal model by introducing a finite delay for the infection mechanism to become effective. Such a delay could be justified by an intermediate incubation state with finite waiting time where the individuals are infected but not yet infectious. We demonstrated that if the incubation time, the recovery time and the basic reproduction number have the appropriate relations, chaotic attractors emerge and persist around the endemic equilibrium.

The present model has a rather large potential of generalizations. One direction of interest may be the extension to multiple compartments in order to explore whether or under which conditions chaos still emerges. On the other hand, the exploration of infection rates exhibiting sudden falloffs with noisy slopes and other parameters may be of interest as well. In this way the effect of natural fluctuations in the implementation of mitigation measures

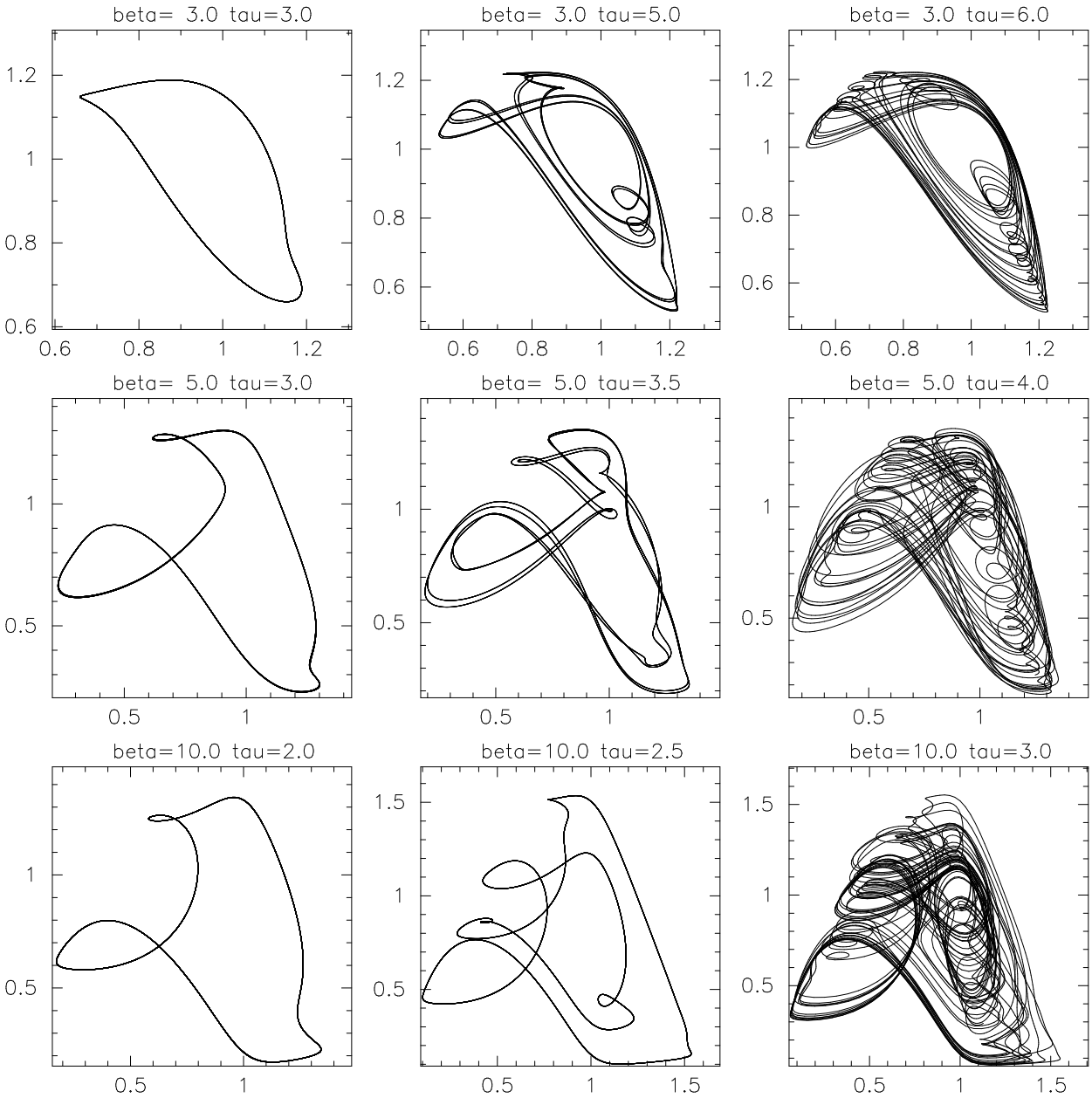

FIG. 10: Numerical solutions of (20) for several values of β and τ, $x(t)$ over $x(t-\tau)$. Chaos occurs earlier for larger values of β. For $\beta < 2$ the limit cycle ceases to exist and the fixed point $x = 1$ remains stable for arbitrary τ.

could be captured.

---

[1] R. T. Malthus, *An Essay on the Principle of Population*, Oxford World's Classics (Oxford University Press, Oxford, 2008).

[2] F. J. Richards, F. J., 'A Flexible Growth Function for Empirical Use', J. Exp. Bot. 10, 290 (1959).

[3] A. J. Lotka, 'Contribution to the Theory of Periodic Reaction', J. Phys. Chem. 14, 271 (1910).

[4] V. Volterra, 'Variazioni e fluttuazioni del numero d'individui in specie animali conviventi', Mem. Acad. Lincei Roma. 2, (1926).

[5] W. O. Kermack, A. G. McKendrick, 'A contribution to the mathematical theory of epidemics', Proc. Roy. Soc. A115, 700 (1927).

[6] R. M. Anderson, R. M. May, *Infectious Diseases in Humans*, (Oxford University Press, Oxford 1992).

[7] H. E. Soper, 'The interpretation of periodicity in disease prevalence', J. R. Stat. Soc. 92, 34 (1929).

[8] W. Liu, A. Levin, Y. Iwasa, 'Influence of nonlinear incidence rate upon the behavior of SIRS epidemiological models', J. Math Biol. 23, 187 (1986).

[9] Y. Tang, D. Huang, S. Ruan, W. Zhang, 'Coexistence of limit cycles and homoclinic loops in a SIRS model with a nonlinear incidence rate', SIAM J. Appl. Math. 69, 621 (2008).

[10] D. Xiao, S. Ruan, 'Global analysis of an epidemic model with nonmonotonic incidence rate', Math. Biosci. 208, 419 (2007).

[11] M. Bestehorn, T. M. Michelitsch, B. A. Collet, A. P. Riascos, A. F. Nowakowski, 'Simple model of epidemic dynamics with memory effects', Phys. Rev. E105, 024205 (2022).

[12] M. Bestehorn, T. M. Michelitsch, 'Oscillating behavior of a compartmental model with retarded noisy dynamic infection rate', Int. J. Bifurc. Chaos Appl. Sci. Eng. 33, 2350056 (2023).

[13] F. A. Rihan, *Delay Differential Equations and Applications to Biology*, (Springer Nature Singapure 2021).

[14] G. E. Hutchinson, 'Circular causal systems in ecology', N.Y. Acd. Sci. 50, 221 (1948).

[15] M. Bestehorn, E. V. Grigorieva, S. A. Kaschenko, 'Spatio-temporal structures in a model with delay and diffusion', Phys. Rev. E70, 026202 (2004).

[16] T. Granger, T. M. Michelitsch, M. Bestehorn, A. P. Riascos, B. A. Collet, 'Four-compartment epidemic model with retarded transition rates', Phys. Rev. E107, 044207 (2023).

[17] D. Mackey, L. Glass, 'Oscillations and chaos in physiological control systems', Science 197, 28 (1977).

[18] M. Bestehorn, *Computational Physics*, De Gruyter Berlin/Boston (2023)

[19] L. Gostiaux, W. J. T. Bos, J.-P. Bertoglio, 'Periodic epidemic outbursts explained by local saturation of clusters', Phys. Rev. E107, L012201 (2023)